International Journal of Scientific Engineering and Technology (ISSN : 2277-1581)
www.ijset.com, Volume No.1, Issue No.4, pg : 111-116 01 Oct. 2012

Plasma Enhanced Chemical Vapor Deposited (Pecvd) Silicon-Rich-Nitride Thin Films For Improving Silicon Solar Cells Efficiency

A. Kumar[1], W.R. Taube[2], R. Sarvanan[3], P.B. Agarwal[4], P. Kothari[5], D. Kumar[6]

[1,2,3,4,5]Sensors and Nanotechnology Group, CSIR-Central Electronics Engineering Research Institute (CEERI), Pilani-333031, India
[6]Electronics Science Department, Kurukshetra University, Kurukshetra – 136119, India
* Corresponding author: akumar1758@yahoo.co.in

Abstract

Silicon-rich-nitride (SRN) films were deposited by plasma enhanced chemical vapour deposition (PECVD) by changing the silane and ammonia flow rates. These films were thermally annealed for precipitation of silicon nanocrystals. Measurements of refractive indices and FTIR absorption spectra of these films indicated increase in the silicon content. Thermally annealed SRN films exhibited photoluminescence in visible region indicating their potential as down-conversion layer for efficiency improvement in solar cells. A significant relative improvement in conversion efficiency using SiO_x/SRN layers in solar cells has been reported in our earlier work. In this paper, we present detailed synthesis process, characterization and analysis of SiN films. Characterization results and solar cell measurements indicate that the observed photoluminescence at 577nm in visible range in selected films along is responsible for improvement in conversion efficiency through down-conversion of high energy solar photons.

Keywords: Silicon-rich-nitride, PECVD, Silicon-nanostructures, Down-conversion, Silicon solar cells, Photoluminescence.

Introduction

PECVD hydrogenated silicon nitride (SiN_x:H) thin films have attracted great attention in silicon solar cell manufacturing due to their excellent passivation and anti-reflection properties [1,2]. Silicon nitride films can be deposited by low-pressure-chemical-vapor-deposition (LPCVD) or plasma enhanced chemical vapour deposition (PECVD) techniques. PECVD is well suited for large area solar cell fabrication due to lower deposition temperature. Properties of SiN_x:H films can be controlled by varying the process parameters namely, flow rate of silane and ammonia gases, deposition temperature and RF power [3]. In recent years, extensive efforts have been made to improve conversion efficiency of silicon solar cells by employing nanostructures and nanotechnologies [4-6]. In one such approach, nanostructures convert higher energy photons into lower energy photons which are absorbed more efficiently by silicon solar cell [7]. Another proposed mechanism for efficiency enhancement is the generation of multiple excitons in quantum dots by high energy photons (> 2 E_g) [8]. Improvement in open circuit voltage (V_{OC}) and short circuit current (I_{SC}) of silicon solar cells have been reported by coating a film of spin-on-glass containing silicon-nanoparticles (SiNP) [9], and silicon nanoparticles' suspension in organic solvent [10]. But, these approaches were not very effective in improving the performance of solar cells, because these films were applied to the cell after fabrication. An effective approach would be the integration of silicon nanoparticles within the solar cell structure. This integration could be done as silicon-rich-oxide (SRO) or silicon-rich-nitride (SRN) films during fabrication process, these films on thermal annealing result in precipitation of silicon nanocrystals [11]. Recently, integratiing silicon nanocrystals in SRO film on crystalline silicon solar cells has shown improvement in internal quantum efficiency (IQE) for high energy photons, but a reduction in overall power conversion efficiency [12]. SRN is a better material system than SRO, due to lower energy barrier between silicon and silicon-nitride compared with silicon and silicon-oxide and requirement of lower annealing temperature [4, 13]. Also, PECVD silicon nitride films provide good surface passivation. Silicon nanocrystals embedded in dielectric matrix are potential materials for next generation silicon solar cells such as tandem, up/downconversion, and multiple exciton generation [14]. The short term objective of these R & D efforts is to improve the efficiency of silicon solar cells with minimum deviation in the existing technology. This has been the motivation of our study on integrating silicon nanocrystals embedded in PECVD SiN_x matrix in the solar cell structure for enhancing the conversion efficiency. Recently, we reported efficiency enhancement in crystalline silicon solar cell with optimized anti-reflection coating (ARC) films embedded with silicon nanocrystals in SiN_x matrix by PECVD[15]. In this paper, we present process development of photoluminescent SRN films by PECVD technique, their characterization and analysis. SRN films with favourable composition and properties for application in solar cells efficiency improvement were integrated in solar cells.

Methodology:

Hydrogenated silicon nitride (SiN_x:H) nitride films were deposited on silicon and quartz substrates by PECVD technique using Oxford Instruments™ Plasma Lab equipment. RF (13.56 MHz) was used to create plasma in parallel-plate configuration. Silane and ammonia were used as precursors for silicon and nitorgen. In the present study only the gas flow rates were varied during deposition while other parameters

were maintained at constant value, temperature 300°C, RF power 120 W, chamber pressure 300 mTorr. System was pumped down to 10^{-3} Torr before deposition. Silicon wafers (2", n- type, <111>, 20-25 Ω-cm, 275 µm thick) and 1"x1" quartz substrates were used for deposition. Substrates were cleaned thoroughly before deposition. The ratio of ammonia to silane flow rate was varied from 10 to 1.14 in order to induce change in the silicon and nitrogen contents in the deposited films, see table 1.

Table 1: Deposition parameters for silicon nitride films.

Sample	Temp. (^{0}C)	Pressure (mTorr)	Power (Watts)	Flow rate (sccm)		Flow rate Ratio
				NH_3	SiH_4	
S1	300	300	120	177	17.6	10
S2	300	300	120	100	17.6	5.68
S3,Q3	300	300	120	50	17.6	2.84
S4,Q4	300	300	120	20	17.6	1.14

Thicknesses of films were ~200nm on quartz substrate (samples Q3,Q4) while ~1.0 on few silicon substrate (samples S1,S2, S3,S4). Refractive index and thickness were measured by prism coupler Metricon2010™ and Talystep™. Thermal annealing of all samples was done at 700°C in nitrogen ambient in Thermco™ furnace. Fourier Transform Infrared (FTIR) spectra of silicon nitride films on silicon substrates were measured before and after annealing in 400-4000 cm^{-1} range by Bruker Tensor37™ at room temperature. Photoluminescence (PL) spectra were measured on annealed silicon nitride films on quartz substrate using Traix 550™ spectrophotometer having a He-Cd excitation laser source of 325 nm, average power of 22 mW falling on a spot size of 1 mm diameter. The emitted light was measured by a IDus420™ photodetector.

These films were integrated in silicon solar cell structures using designed fabrication process reported earlier [15]. In brief, fabrication process involved three levels of photolithography for selective emitter, contact window and front metal patterning, initially a KOH based random texturing was carried out. Two different ARCs were used in fabricating two types of solar cells. First cell was with PECVD SiN_x, as in sample S1 (Refractive Index=1.83 at λ=632.8nm), optimized thickness 83 nm, named as reference cell. Second cell was with thermally annealed SRN ARC as in sample S4 (Refractive Index=2.00 at λ=632.8nm), optimized thickness 76 nm, named as nanostructured cell. The second solar cell with SRN film were annealed at 700°C in nitrogen gas for 30 minutes. The fabricated solar cells is shown in Fig. 1.

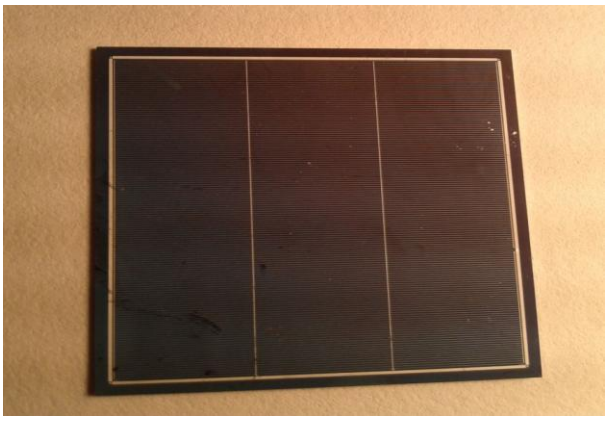

Figure 1 Photograph of fabricated silicon solar cell, size 3cmx3cm [15].

Current density-voltage (J-V) characteristics of fabricated solar cells were measured under AM 1.5G (Air Mass 1.5 Global) insolation source corresponding to 100 mW/cm^2. During measurements, temperature of the solar cells was maintained at 25±1^{o}C through nitrogen and water cooling. The intensity of the source was calibrated using standard photovoltaic reference device.

Results and discussions:

Measured refractive indices for samples with different ammonia to silane flow rate ratio are plotted in figure 2. As NH_3/SiH_4 ratio decreases from 10 to 1.14, value of refractive index increases from 1.83 to 2.00.

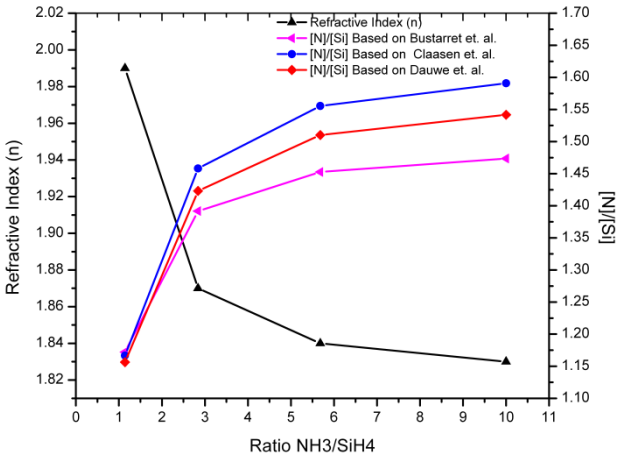

Figure 2 [N]/[Si] ratio and refractive index of the films, as a function of NH_3/SiH_4 flow ratio for samples S1, S2, S3, S4.

The ratio of nitrogen and silicon content ([N]/[Si]) in hydrogenated PECVD amorphous silicon nitride(a-SiN_x:H) films may be estimated by direct methods such as Energy Dispersive Spectroscopy (EDS), Auger Electron Spectroscopy(AES), X-ray Photoelectron Spectroscopy (XPS) or by indirect methods such as using relation between measured refractive indices at a given wavelength and [N]/[Si]

ratio [16-19]. Various equations relate [N]/[Si] ratio with refractive indices as discussed below. Bustarret et. al. [16], gave relation between refractive index (n) and ratio x=[N]/[Si] for PECVD SiN_x:H films given below:

$$n = \frac{n_{a-Si:H} + (3x/4)(2n_{a-Si_3N_4} - n_{a-Si:H})}{1+3x/4} \quad (1)$$

Where, $n_{a-Si:H}$, $n_{a-Si_3N_4}$ are refractive indices of amorphous silicon(3.3), and amorphous silicon nitride(1.9) respectively.

Further, this equation was adapted by Mackel et. al. [17] to estimate the stoichiometry of PECVD SiNx:H films. In Mackel's adapted equation the reported factor of 3/4 is incorrect and the correct factor should be 4/3 which can be easily worked out. So, the correct equation based on Bustarret's relation should be

$$x = \frac{[N]}{[Si]} = \frac{4}{3}\frac{n_{a-Si:H} - n}{n + n_{a-Si:H} - 2n_{a-Si_3N_4}} = \frac{4}{3}\frac{3.3-n}{n-0.5} \quad (2)$$

Another relation given by Claasen et. al. [18], is based on a direct empirical linear fit for different process gases (SiH_4:NH_3:N_2/ SiH_4:NH_3:Ar/ SiH_4:NH_3:H_2) which showed good agreement for all three gas combinations.

$$n = 0.70\frac{1}{x} + 1.39 \quad (3)$$

Dauwe et. al. [19] plotted experimentally measured values of [Si]/[N] reported by Claasen et. al [18], Lauinger et. al.[19], Lenkeit et. al.[19] and gave the following empirical fitting relation:

$$n = 0.74\frac{1}{x} + 1.35 \quad (4)$$

The calculated x = [N]/[Si], ratios using the equations 2, 3 and 4 are plotted in figure 2. It can be seen that as the ammonia flow rate was reduced from 177 sccm to 20 sccm while keeping silane flow rate constant at 17.6 sccm, the value of x decreases to ~1.16. There is a reasonable agreement in the calculated values of [N]/[Si] at refractive index value 2.00. It is shown in the figure that at RI=2.00, the estimated [N]/[Si] ratio is 1.16±0.01 which is less than [N]/[Si] ratio(1.33) in stoichiometric silicon nitride. This indicates that the film is silicon rich. Though, in all these empirical relations for PECVD a-SiN_x:H, hydrogen content may be different due to different process conditions, the predicted [N]/[Si] ratios using the above different relations agreed well with each other at RI=2.00.

FTIR spectra of samples S1, S3 and S4 before annealing, corresponding to [NH_3]/ [SiH_4] ratio of 10, 2.84 and 1.14 are shown in figure 3a. The FTIR spectra exhibits typical peaks corresponding to hydrogenated silicon nitride films. The prominent peaks corresponding to SiN_x:H film before annealing are Si-N asymmetric stretching mode ~870cm^{-1}, Si-N symmetric stretching mode at ~470 cm^{-1}, Si-H_2 stretching mode at ~2250 cm^{-1}, Si-H wagging mode at 650 cm^{-1}, N-H wagging mode at 1150 to 1200 cm^{-1}, N-H stretching mode at ~3380 cm^{-1}. Also N-H_2 bending mode feature is visible at 1550 cm^{-1}. The peaks around 2350 cm^{-1} correspond to CO_2 asymmetric stretching, bending modes and the peaks around 3500 to 3800 cm^{-1} correspond to H_2O symmetric and asymmetric stretching modes. It can also be observed that the Si-N peaks increase as the [NH_3]/[SiH_4] ratio decrease. It may be explained as follows; as the [NH_3]/[SiH_4] ratio is decreased more number of silicon atoms find sufficient nitrogen to bond. But, this trend is expected to change when the [NH_3]/[SiH_4] ratio is decreased significantly such that silicon atoms don't find sufficient nitrogen atom to form Si-N bonds. It can be observed that as the [NH_3]/[SiH_4] flow rate ratio is decreased, the absorbance intensities of Si-H peaks increase while that of N-H peaks decrease.

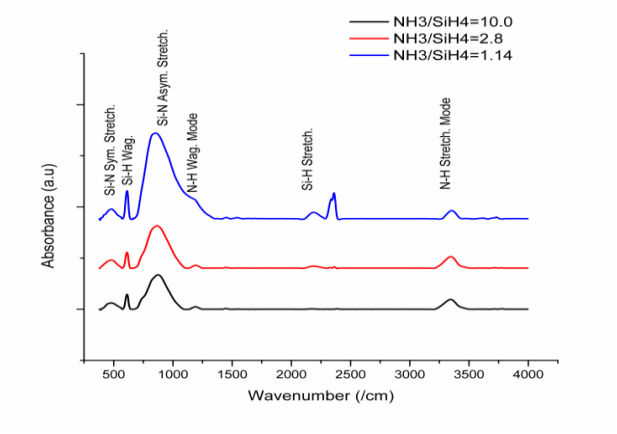

(a)

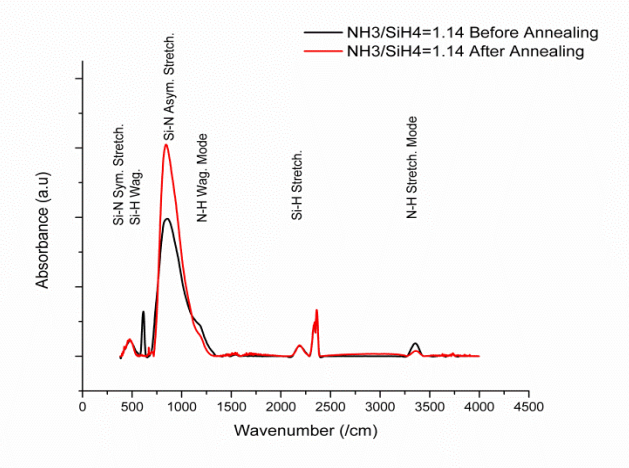

(b)

Figure 3 (a) FTIR absorbance spectra of as-deposited SiN_x:H films (Samples S1, S3,S4) and

(b)SRN film (Sample S4) after thermal annealing.

This could be attributed to the increase in silicon content. FTIR spectra of sample S4 before and after
annealing are shown in figure 3b. After annealing at 700^0C, N-H stretching mode, NH_2 bending mode, N-H wagging mode absorbance, Si-H stretching mode and wagging mode peaks decrease while Si-N asymmetric stretching mode peak increases. The decrease in N-H and Si-H peaks is due to hydrogen evolution during annealing. The broken silicon and nitrogen dangling bonds form Si-N, Si-Si bonds and silicon nanoclusters. The increase in Si-N peaks is evident in the FTIR spectra.

Photoluminescence spectra of samples Q3 and Q4 prepared with NH_3/SiH_4 of 2.84 and 1.14 respectively are shown in figure 4. Sample Q3 showed only a weak broad hump around 430 nm, while sample Q4 exhibited two peaks around 405 nm and 577 nm. Peaks at 405 nm and 430 nm may be ascribed to nitrogen dangling bonds in the deposited film, as also reported by Wang et. al.[20]. Peak around 577 nm in samples Q4 may be due to either band-tail-states in silicon nitride film or quantum confinement of carriers in silicon rich domains (or nanoclusters) which might have formed as a result of phase separation after thermal annealing.

It has been suggested that band tail states recombination results in emission at wavelength greater than 680 nm [21]. In PECVD a-SiN_x:H films, there are in-homogeneities in the stoichiometry. During thermal annealing, silicon-rich and nitrogen-rich phases get separated. The film may be considered as composed of silicon-rich domains in SiN_x matrix. These domains may be of few nm in size [13]. Spatial confinement of photo-generated carriers in these nano-size domains/nanoclusters implies relaxation of selection rules on momentum for radiative recombination, leading to radiative recombination of confined carriers. So, the observed PL peaks at 430 and 405 nm may be attributed to nitrogen dangling bonds and peak at 577 nm may be either due to quantum confinement of carriers in silicon nanodomains/nanoclusters which might have formed after thermal annealing, or recombination at band-tail-states.

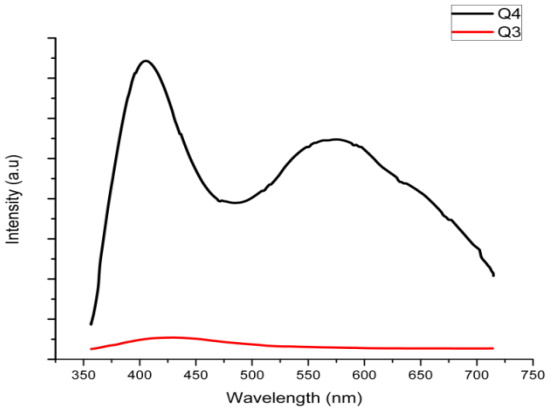

Figure 4: Photoluminescence spectra of SRN film samples Q3 and Q4 after thermal annealing. The broader emission spectra peak is at 577 nm.

For solar cell application, SRN films with deposition parameters corresponding to sample S4 were chosen as ARC. These films were thermally annealed at 700^0C in nitrogen ambient to precipitate silicon nanocrystals. After metal deposition and patterning, sintering was done in forming gas ambient. This forming gas annealing at 450^0C is expected to reduce the traps through hydrogen passivation. These PECVD SRN films exhibiting photoluminescence in visible region are potential material for down-conversion in silicon solar cells. The extracted solar cell parameters from the measured J-V characteristics of reference cell and nanostructured cell are shown in table 2 [15]. It was observed that, nanostructured solar cell has a higher short circuit current density J_{SC} of 35 mA/cm^2 compared to 31.4 mA/cm^2 in reference cell, resulting an improvement of 11.5 %. Similarly, open circuit voltage V_{OC} increased from 0.529 to 0.561 V. The power conversion efficiency of nanostructured solar cell was 14.7% while that of reference cell was 12.7%.

Table 2 Solar cell main parameters extracted from J-V measurements [15].

Solar cell	**V_{OC} (V)**	**J_{SC} (ma/ cm^2)**	**F.F.**	**Efficiency (%)**
Ref. Cell	0.529	31.4	0.77	12.7
NanoStructured Cell	0.561	35.0	0.75	14.7

Thus, there was a relative increase in power conversion efficiency by 12.8%. The observed PL in SRN films (corressponding to sample Q4) in visible range (~577nm) is expected to be responsible for improvement in power conversion efficiency through down-conversion in addition to the surface passivation in fabricated solr cells, also observed by Yuan et. al. using SRO films[12].

Conclusions:

Hydrogenated silicon rich nitride films were deposited with varying [N]/[Si] ratio and thermally annealed to precipitate silicon nanocrystals in the film. PL emission was observed in visible range (577 nm) from thermally annealed silicon rich nitride films. A relative power conversion efficiency enhancement of 12.8% was observed in fabricated nanostructured solar cell with SRN film as an ARC layer compared to a reference cell. This enhancement in conversion efficiency may be attributed to the photoluminescence through down-conversion mechanism and surface passivation. These SRN based ARC are compatible with standard solar cell fabrication process and have direct application in silicon solar cells.

Acknowledgements:

Authors are thankful to Director, CSIR-CEERI, for his support. They are also thankful to the Head, sensors and nanotechnology group for fabrication facilities. The authors would like to thank Dr. P. Misra, RRCAT, Indore for PL measurements. This work has been carried out under Network Project on Nanostructured Advanced Materials funded by Council of Scientific and Industrial Research (CSIR-INDIA), authors gratefully acknowledge the financial support.

References:

[1] L. Cai, A. Rohatgi, S. Han, G. May, and M. Zou, J. Appl. Phys. **83**, (1998), 5885-5889.

[2] J. Schmidt and M. Kerr, Sol. Energ. Mat. Sol. C. **65**, (2001), 585-591.

[3] J. J. Mei, H. Chen, W.Z. Shen, and H.F.W. Dekkers, J. Appl. Phys. **100**, (2006), 073516-1-073516-9.

[4] G. Conibeer, M. Green, R. Corkish, Y. Cho, E. Cho, Chu-Wei Jiang, T. Trupke, B. Richards, A. Shalav, and K. Lin, Thin Solid Films **511**, (2006), 654-662.

[5] A. Nozik, Physica E **14**, (2002), 115-120.

[6] J. De la Torre, G. Bremond, M. Lemiti, G. Guilot, P. Mur and N. Buffet, Thin Solid Films **511-512** , (2006), 163-166.

[7] T. Trupke, M.A. Green, and P. Wurfel, J. Appl. Phys. **92**, 1668 (2002), 1668-1674.

[8] M.C. Beard, K.P. Knutsen, P.Yu, J.M. Luther, Q. Song, W. K. Metzger, R. J. Ellingson and A. Nozik, Nanoletters **7** , 2506 (2007), 2506-2512.

[9] V. Svreck, A. Slaoui, and J.C. Muller, Thin Solid Films **451-452**, 384 (2004), 384-388.

[10] M. Stupca, M. Alsalhi, T. Al saud, A. Almuhanna, and M.H. Nayfeh, Appl. Phys. Lett. **91**, 063107 (2007), 063107-063110.

[11] L. Pavesi and R. Turan (Eds.), Silicon Nanocrystals: Fundamentals, Synthesis and Applications, Wiley-VCH Verlag GmbH, Berlin, 2010.

[12] Z. Yuan, G. Pucker, A. Marconi, F. Sgrignouli, A. Anopchenko, Y. Jestin, L. Ferrarion, P. Bellutti, L. Pavesi, Sol. Energ. Mat. Sol. C. **95**, 1224 (2011), 1224-1227.

[13] L. Dal Negro, J. H. Yi, and L. C. Kimerling, S. Hamel, A. Williamson, and G. Gallib, Appl. Phys. Lett. **88**, (2006), 183103-183106.

[14] M. A. Green, Third Generation Photovoltaics: Advanced Solar Energy Conversion, Springer, 2006.

[15] W. R. Taube, A. Kumar, R. Saravanan, P. B. Agarwal, P. Kothari, B. C. Joshi, D. Kumar, Sol. Energ. Mat. Sol. C. **101**, (2012), 32-35.

[16] E. Bustarret, M. Bensouda, M. C. Habrard, J.C. Bruyere, S. Poulin, S. C. Gujrathi, , Phys Rev. B 8171 (1988), pp. 8171-8184.

[17] H. Mackel and R. Ludemann, J. Appl. Phys **92**, 2602 (2002), pp. 2602-2609.

[18] W.A.P. Claasen, W.G.J.N. Walkenberg, F.H.P.M. Habraken, Y. Tammingo, J. Electrochem. Soc. **130**, 2419 (1983), pp. 2419-2423.

[19] S. Dauwe, Ph. D. Thesis, University of Hannover, Germany, 2004.

[20] M. Wang, D. Li, Z. Yuan, D. Yang, and D. Que, Appl. Phys. Lett. **90**, 2419 (2007), pp. 2419-2423.

[21] M. Molinari, H. Rinnert, M. Vergnat, J. Appl. Phy. **101**, 123532 (2007), 123532-1 – 123532-10.

International Journal of Scientific Engineering and Technology (ISSN : 2277-1581)
www.ijset.com, Volume No.1, Issue No.4, pg : 111-116 01 Oct. 2012

International Journal of Scientific Engineering and Technology (ISSN : 2277-1581)
www.ijset.com, Volume No.1, Issue No.4, pg : 111-116 01 Oct. 2012